Experimental study of the energy-band structure of porous silicon

O. K. Andersen and E. Veje
Oersted Laboratory, Niels Bohr Institute, Universitetsparken 5, DK-2100 Copenhagen, Denmark
(Received 5 September 1995; revised manuscript received 23 January 1996)

Porous silicon samples consisting of either as-grown films, annealed films, or powders have been studied with photoluminescence, (10–700 K) and photoluminescence excitation. In addition, absorption measurements have been carried out on powder. Results are presented and discussed in terms of current models for the luminescence properties of porous silicon. The conclusion is, that for the samples produced and studied here, the luminescence is of molecular nature. From the data, an energy-level diagram related to the luminescence is constructed, and the nature of the band structure is discussed. Of all models proposed for the photoluminescence properties of porous silicon, our data are compatible only with a recently proposed model based on oxygen-related centers. [S0163-1829(96)00120-8]

I. INTRODUCTION

Crystalline silicon (*c*-Si) is an indirect-gap semiconductor, and therefore, luminescence from bulk *c*-Si, based only on electric dipole transitions, is not allowed due to conservation of linear momentum. Consequently, elemental silicon of bulk properties is not well suited for the production of optoelectronic devices. However, silicon is the material most used for the production of electronic components, and therefore, several attempts have been made to modify silicon in one way or another, to circumvent the problem of weak photon emission, related to its indirect band gap. A few years ago it was discovered that it is possible, by etching *c*-Si electrochemically in hydrofluoric acid, to modify the surface, so that it can emit bright photoluminescence (PL) in the visible and near infrared, even at room temperature.[1,2] Electron microscopy studies revealed that such a surface consists of a network of pores and/or columns, and consequently, it has been named porous silicon (PS).[3]

Since then several experimental works have been carried out in trials to understand the PL emission, and various models have been proposed to rationalize experimental data sets. For reviews, see, e.g., Refs. 4–7, and references therein. A large volume of experimental data is available in the literature, with various diversities. Thus, it is not yet clear, whether the bright PL of PS can be related to quantum confinements[8] caused by spatial restrictions, amorphous silicon luminescence,[9,10] or the presence of one or more chemical compounds such as, e.g., polysilane[11,12] or siloxene.[13] Recently, a direct correlation between presence of oxygen-related centers and the intensity of red PL from as-grown and oxidized PS (Refs. 14 and 15), as well as from oxidized silicon nanoclusters[16] has been established. Thus, among all models proposed for the PL properties of PS, this oxygen-defect-based model[14,15] seems to be the most promising one. However, it must be born in mind, that because PS is not necessarily a very clean and well-defined material, the luminescence may be related to a combination of different sources. As a consequence, some of the diversities published may be related to the specific sample production and preparation, because different samples, produced by different investigators, need not be very similar.

Besides the technological interest in PS, there is also considerable interest in PS from a viewpoint of basic research. Therefore, we have found it worthwhile to develop a highly reproducible technique based on electrochemical etching, to produce PS that is homogeneous over a relatively large area, with the purpose of studying such PS with a combination of different optical techniques and also structural techniques such as electron microscopies and secondary-ion-mass spectroscopy.

II. EXPERIMENT

In Fig. 1 is shown a cross section of the electrolytic cell in which the electrochemical etching was carried out. The PS was produced on the anode, which in all of this work was a *p*-type *c*-Si wafer with crystal orientation (100). Wafers with doping levels from 0.005 Ω cm to 30 Ω cm were used. As cathode was used, a corresponding *n*-type *c*-Si wafer, 10 Ω cm, which could be used several times, since it was not exposed to hard wear. The distance between the electrodes was 20 mm. The two aluminum flanges on the back sides of the silicon electrodes served two purposes, namely (i) to support the silicon wafers in a uniform way so that they could be pressed against the sealing *O* rings of rubber, without breaking, and (ii) to give good electric contacts to all of the back side of each Si electrode, ensuring that the current density and thus the etching rate was constant all over the surface exposed to the HF. Actually, we always observed a very uniform PS formation, except at the rim of the exposed region of the anode, where the degree of etching always appeared to be slightly increased.

Constant current densities ranging from 10 mA/cm^2 to 60 mA/cm^2 were employed for different lengths of time. After etching with HF, the samples were always flushed with distilled water. The PS layer could be oxidized anodically in the same electrolytic cell, using a KNO_3 electrolyte. With a current density around 20 mA/cm^2 and for etching times of the order of one hour, a thick layer of PS was formed. Scanning electron microscopy investigations revealed a typical thickness of around 30 μm. Depending on the doping level of the substrate, PS powder was released from the wafer, but remained at the wafer surface. This phenomenon was observed

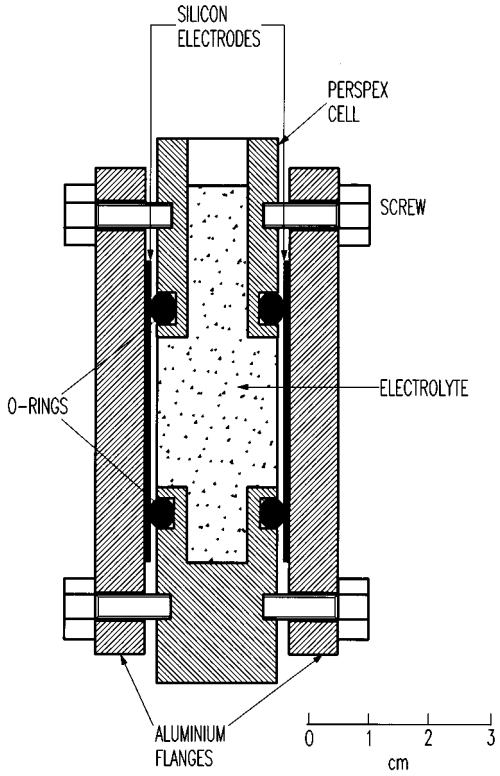

FIG. 1. Cross section of the electrolytic cell used for the production of PS. The different parts are on the same scale, except for the thicknesses of the silicon electrodes, which are exaggerated to make them visible.

primarily for resistivities around 2 Ω cm. After rinsing with H_2O and drying in air, the powder could be wiped off the surface, on which it had been produced, and sufficient amounts of powder could be produced to study its properties. A comparison between data obtained from the bare powder with corresponding results from the PS film remaining on the wafer, and produced together with the free powder, makes it to some extent possible to identify possible influences from the unetched silicon, as well as from that part of the PS layer on the wafer, where the etching processing has not terminated.

Traditionally, a platinum wire is used as cathode, but here, this was substituted with an *n*-type Si wafer (cf. Fig. 1) to obtain a more homogeneous electric field in the electrolyte leading to samples with very uniform surfaces (except for the rim, as mentioned above). Introductory attempts in which a platinum wire was used as cathode resulted in samples with rather inhomogeneous surfaces.

The samples have been studied with PL, photoluminescence excitation (PLE), and for powders also with absorption measurements. The light of interest was dispersed with a one-meter scanning spectrometer (McPherson model 2051) with a ruled grating blazed at 1000 nm, and detected with either a photomultiplier (Hamamatsu model R943-02), using single-photon counting (wavelengths below approximately 900 nm), or a germanium diode (North Coast Scientific Corporation model EO-817L), using a lock-in technique (800–1700 nm).

The overall quantum efficiency of the spectrometer with detecting device has been determined as described in Ref. 17, with the use of a coiled-coil filament lamp standard of spectral irradiance (Optronic Laboratories model L-97). All spectra have been corrected for the variation in quantum efficiency as a function of the detecting wavelength. Appropriate filters were used to sort out different spectral orders and also to remove stray light. The light sources used in the PL measurements, were a red HeNe laser (633 nm), a green HeNe laser (543 nm), an argon-ion laser (488 nm), or a filtered Hg spectral lamp (254 nm).

The light source used for the PLE measurements, was a stabilized 250-W filament lamp coupled to a 0.67-m scanning spectrometer (McPherson model 207), with a ruled grating blazed at 1000 nm. The coupling of light from the lamp to the spectrometer and also from the spectrometer to the sample was done with the use of optical fiber cables. Also here, appropriate filters were used to sort out different spectral orders. The resulting outcoming photon fluence was measured versus wavelength with the quantum-efficiency calibrated one-meter spectrometer described above. In all of the PLE spectra given in the following, data points have been normalized to same number of exciting photons.

The samples could be mounted strain free in a closed-cycle helium refrigeration system and studied from 10 to 300 K. Also, they could be heated from room temperature to 700 K.

III. RESULTS

A. Sample preparation conditions and structural properties

Strong PL signals have previously been observed at wavelengths from the near infrared through the visible to the blue, and the spectral features have been reported to depend on the sample porosity, etching conditions, and also surface chemical treatment like, e.g., oxidation, for an overview, see, e.g., Ref. 4 and references therein. Therefore, we have varied the sample production parameters to study such possible effects. However, we observed almost the same relative spectral shape in PL, independent of etching current density (from 10 mA/cm^2 to 60 mA/cm^2), etching time (from a few minutes to more than two hours), hydrofluoric acid concentration (10–40 %), addition of ethanol to the etch bath, oxidation with KNO_3, and doping level (0.005–30 Ω cm). These investigations were all carried out on *p*-type (100) *c*-Si. Naturally, the PL intensity was found to depend on the current density and etching time, but in all cases, the PL intensity maximum occurred close to 730 nm for free PS powder and mainly around 780 nm for PS films remaining on the wafers, when the argon-ion laser (488 nm) was used for excitation. Thus, our conclusion here is, that with our method to produce PS, the PL spectral shape depends not very much on production parameters. To the eye, the color of the film samples ranged from yellow-green to reddish-brown. Nonetheless, the relative PL spectral distributions were remarkably similar. The visually different colors are most presumably related to interference phenomena. The PS powder always looked reddish-brown and, when inspected with a microscope, glassy.

For simplicity, in all of the following, PS powder freed from the wafer, on which it has been produced shall be referred to as PS powder, whereas PS remaining on the wafer

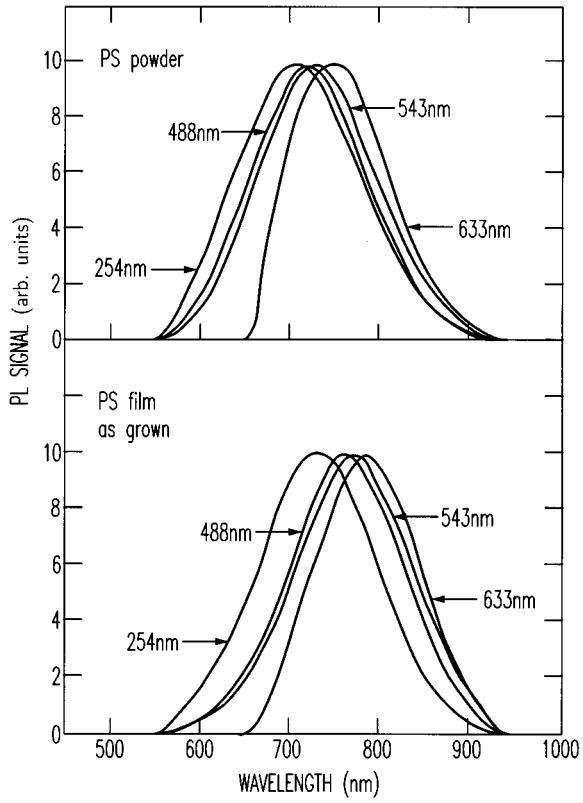

FIG. 2. PL spectra for PS powder (upper section) and as-grown PS film (lower section), obtained at room temperature and with four different light sources, the wavelengths of which are indicated in the figure.

shall be denoted as PS film. Typical PL spectra obtained at room temperature are shown in Fig. 2 for PS powder (upper section) and for PS film (lower section). The powder and the film were produced together. For both samples, four PL spectra are shown, obtained with four different excitation wavelengths, as indicated in the figure. As seen, for each sample, the position of the maximum shifts slightly towards longer wavelengths, with increasing excitation wavelength. Also, for same excitation wavelength, the position of the maximum for the powder is located at a slightly shorter wavelength than for the PS film. However, all spectra in Fig. 2 span the same wavelength interval 560–940 nm, independent of excitation wavelength (except the two spectra obtained with the red HeNe laser, which for obvious reasons are not extended as much towards shorter wavelengths as the other PL spectra are). The shift with excitation wavelength in the position of the maximum is not followed by an identical shift of the whole PL spectrum.

With the Hg lamp as excitation source, a very careful search for PL in the blue region was carried out, but the result was negative. No matter how the sample was prepared and treated, no PL component could be observed at shorter wavelengths than what is seen in Fig. 2.

Besides the bright PL in the wavelength region approximately 600–900 nm, as shown in Fig. 2, also a weak band with maximum at around 1200 nm has previously been reported.[18] Therefore, we also searched carefully for PL in the wavelength region 900–1700 nm, but failed to observe anything. The relative detection sensitivity in this wavelength region (remembering that the Ge diode had to be used instead of the photomultiplier counting individual photons) was such that a PL signal with photon fluence 10^{-4} times that of the 600–900-nm band would safely have been observed. In this search, the use of filters which entirely rejected any second-order light was mandatory.

The chemical composition of a selection of samples was studied with secondary-ion-mass spectroscopy (SIMS) with the use of 0_2^+ and Cs^+ projectiles. Scans for positive, as well as negative secondary ions, were carried out. The SIMS spectra indicated that the samples contained hydrogen, oxygen, fluorine, and silicon. In addition, traces of the following impurities, carbon, nitrogen, sodium, and chlorine were seen.

The structure of a series of samples grown under different conditions was studied with a scanning electron microscope, revealing spongelike structures similar to what has been reported several times previously, see e.g., Refs. 19–25. Powder samples were studied with transmission electron microscopy in a search for crystalline structure of PS. The result was negative, with the conclusion that our PS either is amorphous or consists of microcrystallites of size below 30 nm. No trace of a diffraction pattern similar to that obtained from c-Si was seen from the PS.

Some PS powder was mechanically crushed as much as possible in a mortar. PL spectra obtained from the finely pulverized PS were identical to those obtained before the crushing was carried out.

Some samples were studied with PL shortly after they had been produced. Then, they were stored several weeks in air and revisited. The ageing did not change the spectral shape obtained from PS powder appreciably, and only small shifts towards shorter wavelengths were observed for PS films.

If a sample was illuminated with a high irradiance, the PL intensity was observed to change in time similarly to what is reported in Ref. 26. Such illumination-dependent intensity variations in time will distort a PL spectrum, if the spectrum is scanned slowly, while the sample is exposed to a high irradiance. Therefore, all of the results reported here have been obtained under such conditions that the spectral distortions during the measurements could safely be ignored. This condition could easily be fulfilled, due to the very bright PL signals.

B. PL intensity and spectral distribution versus sample temperature

For the PS powder, the relative spectral distribution was almost independent of the sample temperature T, see Fig. 3, in which PL spectra obtained at different temperatures and normalized to the same height are shown. Note especially in Fig. 3, that the position of the maximum and also the half width are independent of T. The total PL intensity decreased steadily with increasing T, see Fig. 4, upper section, in which the integrated PL intensity is plotted versus T. In this figure, the data have been fitted with a relation of the form

$$I(T)=I_0[1+a\ \exp(-E_A/k_BT)]^{-1}, \tag{1}$$

where E_A is an activation energy, k_B is Boltzmann's constant, and I_0 and a are constants, for details, see Ref. 27. As seen in Fig. 4, the data below 300 K can be reproduced satisfyingly well with the relation given in Eq. (1). The value

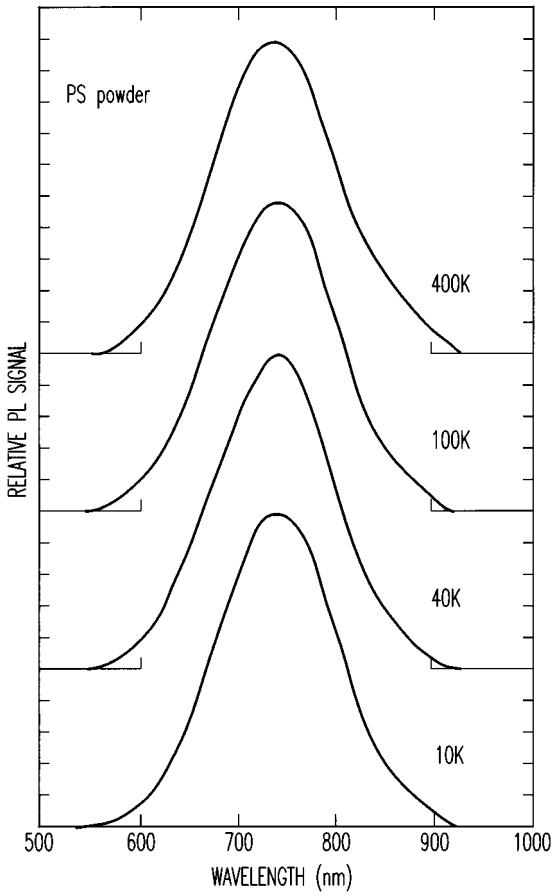

FIG. 3. PL spectra obtained from PS powder at different temperatures, as indicated. An argon-ion laser (488 nm) was used as a light source. The spectra have been normalized to the same height.

obtained for E_A for the PS powder was (0.07 ± 0.01) eV. For prolonged heatings at temperatures above $\sim$500 K, the PS powder degraded in an irreproducible way. However, if the powder was kept below such temperatures, the PL spectra could be retained at all temperatures.

Contrary to the PS powder, for as-grown PS films, the spectral distribution depends remarkably much on T in the region 10–80 K, see Fig. 5, in which spectra obtained at different temperatures have been normalized to the same height. Above $T\cong80$ K, the relative spectral shape was essentially independent of T, cf. Fig. 5. Besides these changes in relative PL spectral shape, the integrated PL intensity also changed noticeably with T. This is shown in Fig. 4, lower section. Also for PS films, irreproducible degradation was observed for prolonged heatings at temperatures above approximately 500 K. However, if a film had been heated to around 600 K for approximately one hour, then the PL spectra observed at all temperatures, including temperatures below 80 K, resembled those emitted from PS powder, i.e., finer structures like those depicted in Fig. 5 became absent, and instead, very smooth relative spectral distributions were seen at all temperatures, see Fig. 6. In the upper section of Fig. 4 is plotted the change in total PL intensity versus T (triangles) together with similar data for PS powder (crosses).

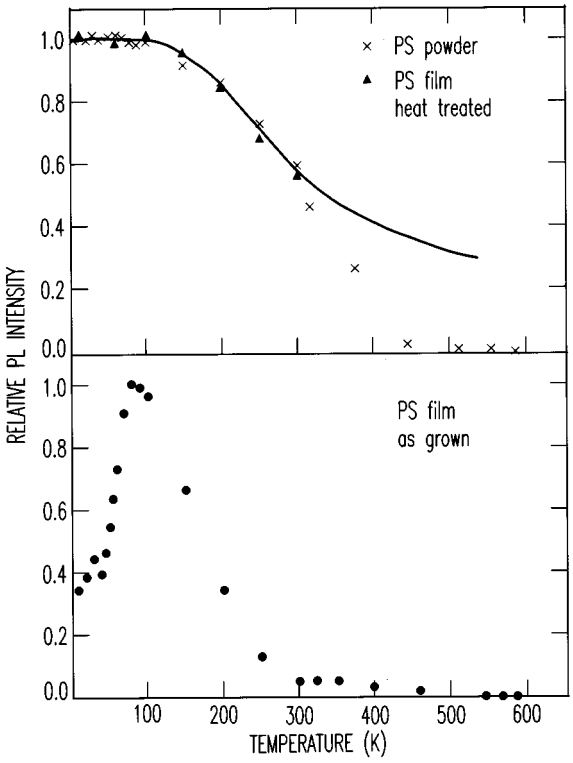

FIG. 4. Total PL intensity as a function of the sample temperature for PS powder and heat-treated film (upper section), and for as-grown PS film (lower section). The curve shown in the upper section has been obtained by fitting Eq. (1) to the powder data. An argon-ion laser (488 nm) was used as a light source.

C. Photoluminescence excitation and absorption results

PLE measurements were carried out at several detection wavelengths for PS powder as well as PS film. In Fig. 7 are shown typical results obtained at room temperature. As seen from this figure, for each sample there is a threshold for the excitation. In Fig. 8, the measured threshold energies are plotted versus the detection energy for PS powder (crosses), for an as-grown film (filled circles) and also for a PS film, which was heated to 600 K for one hour before the PLE measurements were carried out (filled triangles). In this figure, two straight lines with slope one are drawn, which fit the high-energy points of the data sets, and also two horizontal lines, which fit the low-energy data for the PS powder and the as-grown PS film, respectively. As seen, for PS powder, the threshold is (1.59 ± 0.01) eV, independent of the detection energy below (1.52 ± 0.01) eV, whereupon it increases linearly with detection energy. In this region, the constant difference between detection energy and the corresponding threshold energy is (0.07 ± 0.01) eV. Similarly, for the as-grown PS film, the threshold has the constant value (1.71 ± 0.01) eV for detection energies below (1.57 ± 0.01) eV, and above this value, it increases linearly with increasing detection energy. Here, the constant difference between detection energy and the corresponding threshold energy is (0.14 ± 0.01) eV. For the heat treated film, the high-energy points fall close to the points for the as-grown PS film, whereas the low-energy points fall close to those obtained with the PS powder.

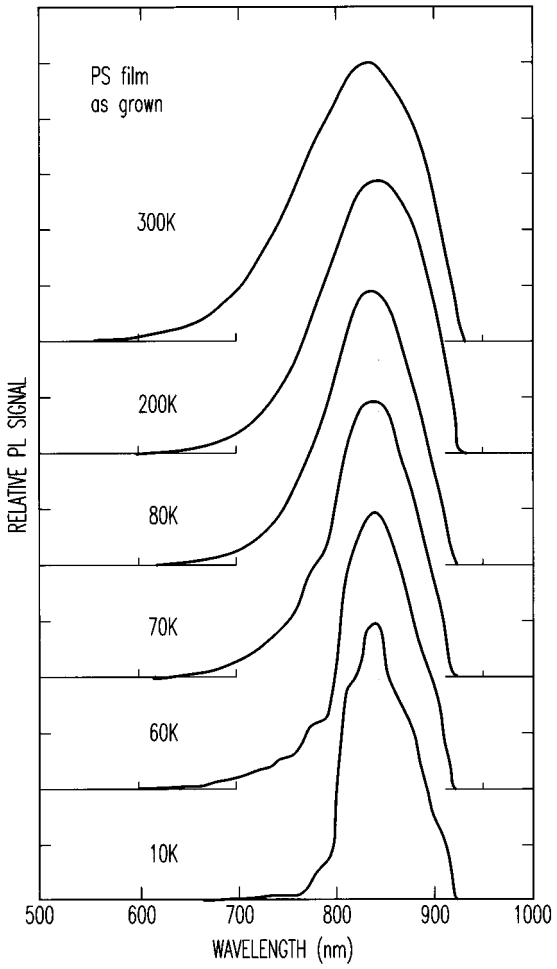

FIG. 5. PL spectra obtained for an as-grown PS film at different temperatures, as indicated. An argon-ion laser (488 nm) was used as a light source. The spectra have been normalized to the same height.

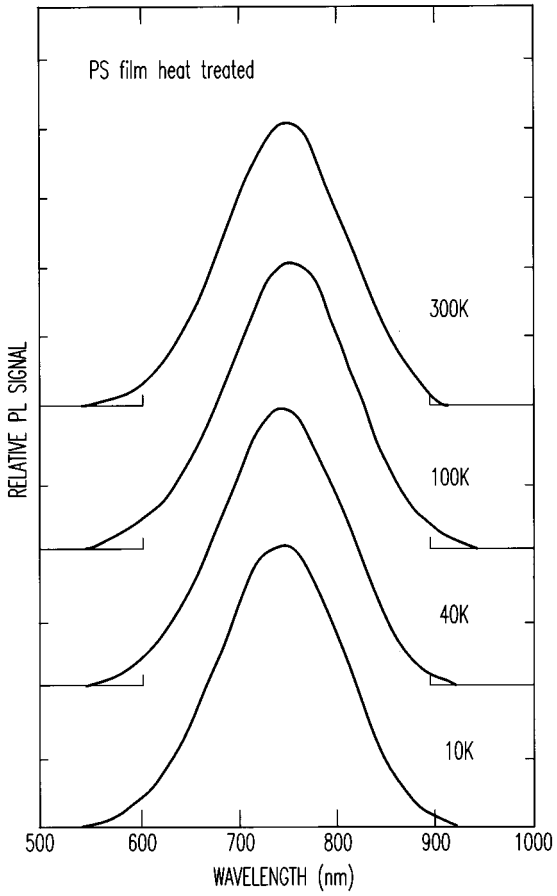

FIG. 6. PL spectra obtained from a heat-treated PS film at different temperatures, as indicated. An argon-ion laser (488 nm) was used as a light source. The spectra have been normalized to the same height.

In Fig. 9 is shown an absorption spectrum for PS powder. The onset for absorption is located at (780±5) nm, corresponding to a photon energy equal to (1.59±0.01) eV.

IV. DISCUSSION

The discussion given in the following and also the conclusions are primarily related to, and also limited to the above-presented results. This is because PS produced elsewhere may possess properties somewhat different from what we have been working with. We shall first mainly discuss the results obtained with PS powder. Then, the results obtained from the as-grown PS films, as well as heat-treated films will be discussed.

As mentioned in the introduction, one of the models to explain the bright PL from PS is based on existence of geometrically small, well-confined regions. A small structure will enhance the emission intensities, because electrons and holes are confined spatially. In addition, a series of localized quantum states is formed, the energies of which increase with decreasing size of the confinement region. For a detailed theoretical account, see Ref. 28. It has been estimated,[8] that for silicon, particles with sizes below approximately 5

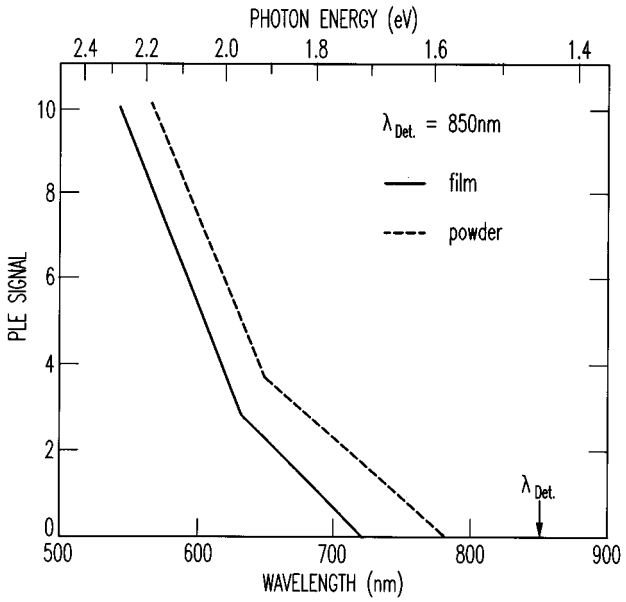

FIG. 7. Typical PLE spectra obtained at room temperature for PS powder and as-grown PS film from the same growth. The detection wavelength was 850 nm.

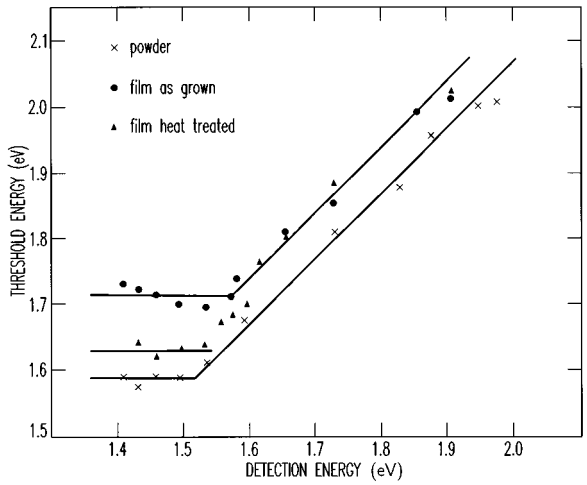

FIG. 8. PLE threshold energies plotted versus detection energy for PS powder (crosses), as-grown PS film (circles), and heat-treated PS film (triangles). The data have been fitted with horizontal lines together with lines with slope unity.

nm would increase the band-gap energy to the interval 1.5–1.9 eV, which is needed to account for the PL spectral distributions shown in Fig. 2. At the same time, the oscillator strengths would be enhanced noticeably, as is required to account for the overall PL intensities. For structures of geometrically same size, narrow line radiation would result. Thus, the broad spectral features seen in Fig. 2 would indicate the presence of a broad distribution of particle sizes. This is no surprise, remembering the etching technique used to produce PS. For such a system, it is difficult to predict theoretically how the resultant PL spectral distribution would change with sample temperature, but it does not seem possible to account for the fact, that we observe essentially no relative variation in the PL spectral distribution with temperature, cf. Fig. 3. Especially, it is worth noting that the

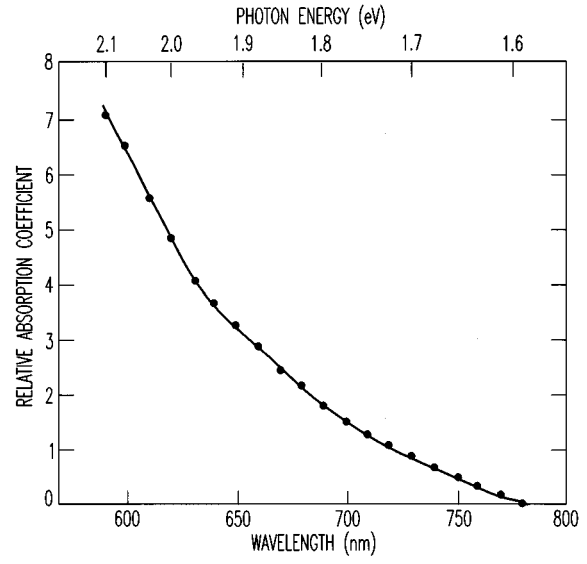

FIG. 9. Relative absorption coefficient for PS powder plotted versus the wavelength of the light (lower scale) and also the photon energy (upper scale).

temperature variation of the increase in band-gap energy introduced by any spatial confinement must follow the temperature variation of the band-gap energy for silicon, which is reduced by 0.13 eV when the temperature is raised from 0 K to 600 K, see Ref. 29. With the argon-ion laser (488 nm) used for excitation, we observe for all temperatures, that the PL maximum is located at ~730 nm, corresponding to a photon energy of 1.72 eV, and also that the PL spectra are extended from ~560 nm (2.21 eV) to ~940 nm (1.32 eV) independent of sample temperature, cf. Fig. 4, as well as excitation energy. A systematic reduction of 0.13 eV would correspond to a wavelength shift of the maximum to roughly 790 nm, which would easily be seen (cf. Fig. 3).

The relative shape of our PL spectra was not noticeably influenced by etching conditions, cf. Sec. III A. This too, is difficult to account for with the confinement model, because it is well established that etchings carried out with high current densities and for long times lead to higher porosity with reduced particle size, as compared to etchings done with small current densities and for short times. However, we observed no blueshift of the PL spectra from heavily etched samples, as compared with PL from lightly etched samples.

Thus, based on our experimental data and from the above discussion, we conclude that it seems quite problematic to account for our experimental results with the confinement picture. This need not be a surprise, because according to that model, particle sizes of approximately 5 nm or below, would be needed, and for such small silicon particles, the electronic energy properties would be strongly influenced by surface contamination. The surface of silicon is chemically very active. Among other things, it is well accepted that the surface of as-prepared PS is saturated with SiH_x (Ref. 29), and also that the surface of silicon stored in air will oxidize rapidly.

Recently, Prokes and Glembocki[30] used intense laser irradiation to anneal a PS sample, and once annealed, the PL from the sample exhibited no energy shift in the temperature interval 300–1100 K. They arrived at the same negative conclusion as we have given above, namely, that the PL cannot be the property of Si nanoparticles. This is worth noting, because their work differed from ours in choice of temperature interval (they measured from 300 to 1100 K, whereas we have been working from 10 to 700 K), and also in choice of sample preparation. Our samples were first studied below room temperature and then brought to elevated temperatures, whereas they studied samples which had been annealed at 1100 K. Actually, they observed that the annealing itself shifted the PL maximum from approximately 1.5 to 1.72 eV, but once shifted, it remained at 1.72 eV, which is very close to the position of the maxima in Fig. 3. They interpreted their data in terms of the oxygen-defect-based model,[14,15] which consequently may well be applicable to our data too, a point we shall return to later.

The temperature dependence of the band-gap energy of amorphous silicon is even larger than that for c-Si.[31] In accordance with that, the PL spectrum from amorphous hydrogenated silicon is known to shift considerably with sample temperature.[32] Thus, models based on assumption of presence of amorphous silicon have the same difficulties as those outlined above for c-Si.

The above-discussed temperature invariance of the PL

spectra for PS powder is on the other hand compatible with a molecular origin of the PL. As a possible candidate for such molecular luminescence, siloxene has been suggested and studied in some detail. Siloxene, of stoichiometry $Si_6O_3H_6$, has a PL spectrum which peaks at around 550 nm (Refs. 33, 34), slightly depending on the preparation. Thus, as-prepared siloxene seems not to be the right candidate for the PL observed here. This is in agreement with the work presented in Ref. 35, in which siloxene, SiO_2, Si, and PS were studied with x-ray-absorption fine-structure measurements, which revealed a very reduced content of oxygen in PS, as compared with siloxene and SiO_2. In passing, we mention that whereas dry siloxene reacts violently with air,[36] all our samples have been stored in air from when they were grown, and they have remained stable in air. That in itself precludes that they should be composed purely of siloxene.

By annealing siloxene, the PL maximum is shifted towards longer wavelengths, so that a substantially better agreement with the spectra shown in Fig. 3 is obtained.[33,37–39] Also, as-prepared siloxene has the absorption edge at 2.5 eV,[40] which is substantially above the 1.59 eV found here (see Sec. III C), but by annealing siloxene, the position of the absorption edge is moved towards lower energies, depending on the annealing temperature. By annealing at 700 K, an absorption edge almost identical to that shown in Fig. 9 is observed.[40] Still, agreement between PLE spectra for siloxene reported[38] and those seen here (Fig. 7) is not convincing. Furthermore, according to Ref. 39, the annealed material consists of an amorphous Si:O:H alloy, which has little correlation to the ordered siloxene compounds. Thus, the better agreement between annealed siloxene and the PS powder may probably indicate that the PS powder has some relation to some Si:O:H alloy, but not to the ring structure of siloxene. In addition, two problems exist, namely, (i) that for siloxene, the ratio of silicon atoms to oxygen atoms remains as 2:1, independent of the annealing,[40] and according to Ref. 35, the content of oxygen in PS is much below that in siloxene. Also, (ii) the SIMS measurements we carried out, indicated the presence of fluorine in our samples, and this element is not a constituent of siloxene.

Although we are unable to specify a chemical species responsible for the PL observed from PS by comparing our data to data in the literature, it is possible to sketch the energy diagram related to the PL observed here, as follows. The absorption edge (1.59 eV) seen in Fig. 9, is equal to the minimum photon energy (1.59 eV) required to excite PL, as seen from the position of the horizontal line for PS powder in Fig. 8. Consequently, excitation resulting in PL takes place into a band, the bottom of which is situated 1.59 eV above the highest occupied molecular orbital (HOMO) in PS powder. According to the absorption measurements, as well as the PLE data, the band is continuously extended at least up to the upper limit of photon energies used here, 3.1 eV. This band is drawn to the left in Fig. 10, in which it is separated from the HOMO with the band-gap energy E_1.

In PL, with all excitation energies larger than 2.28 eV, all PL spectra observed span the photon energy interval 1.32–2.21 eV, and the position of the intensity maximum moves only slowly towards higher energies for increasing photon energy, cf. Sec. III A. This indicates that the PL results from

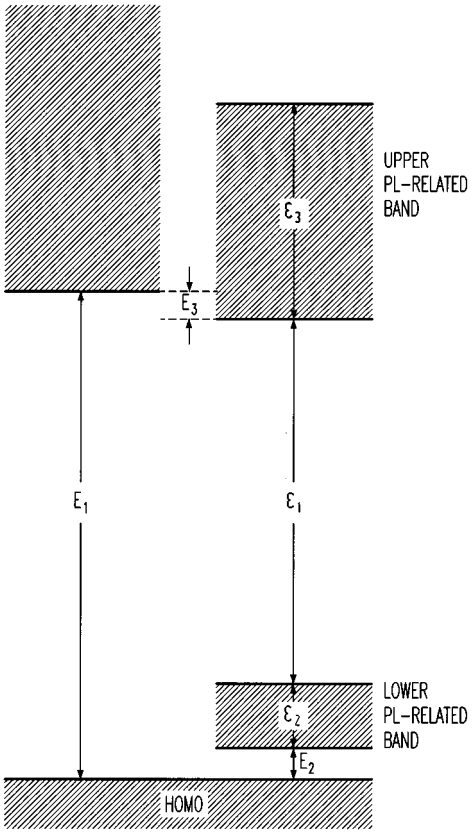

FIG. 10. Energy-band-structure diagram for PS. The values obtained for the different energies sketched in this figure are given in Table I.

band-to-band radiation, with a maximum energy separation of 2.21 eV, and a minimum separation of 1.32 eV. It is, in principle, possible that more than two bands are involved. However, for all photon excitation energies, the resulting PL spectrum has only one broad maximum with no minima and secondary maxima, shoulders or the like. Therefore, it can be assumed here that the PL results as radiative recombinations from one upper band to one lower band. In the following, these two bands will be referred to as the upper PL-related band and the lower PL-related band, respectively. They are drawn to the right in Fig. 10.

If the bottom of the lower PL-related band is not separated from the HOMO (i.e., setting $E_2=0$ in Fig. 10), then some absorption and also PLE for the longest detection wavelengths should be seen below 1.59 eV, but that is not the case, cf. Figs. 8, 9. This indicates that the bottom of the lower PL-related band is above the HOMO, i.e., in Fig. 10, $E_2\neq 0$. It is possible that the bottom of the upper PL-related band is located below the E_1 band edge, but not above.

From the position of the line with slope one in Fig. 8 for PS powder, it is seen that to excite PL of photon energies above 1.52 eV requires an excitation energy surpassing the detection energy by 0.07 eV. If electrons excited above the band gap E_1 (to the left in Fig. 10) can be transferred to the upper PL-related band (to the right in Fig. 10), without relaxing their energy before they undergo radiative decay to the lower PL-related band, then, the above-given energy difference of 0.07 eV can be identified as equal to E_2 in Fig. 10. At the same time, the band-edge difference E_3 in Fig. 10 is

TABLE I. The table lists the values for the energies shown in Fig. 10. For the deduction of the values listed, see the text.

	PS powder	PS film as grown
E_1 (eV)	1.59±0.01	1.71±0.01
E_2 (eV)	0.07±0.01	0.14±0.01
ε_1 (eV)	1.32±0.01	1.32±0.01
ε_2 (eV)	0.20±0.02	0.25±0.02
ε_3 (eV)	0.69±0.02	0.64±0.02

identified as being equal to zero.

The Fermi level is thought to be above the HOMO band and below the lower PL-related band, i.e., in the band gap of energy E_2. The activation energy E_A=0.07 eV, as deduced from the intensity versus temperature dependence, cf. Sec. III B and Fig. 4, can be interpreted as the energy difference between the HOMO and the bottom of the lower PL-related band, the reduction in PL intensity seen by increasing the temperature being caused by thermal excitation of electrons from the HOMO to the lower band. Also, this leads to E_2=0.07 eV. However, although such a consideration agrees with the above-given result for E_2, it cannot be regarded as a strict confirmation of it, remembering the relatively large uncertainty related to E_A and also, that the fitting of Eq. (1) to data in Fig. 4 is satisfyingly good only for temperatures below 300 K.

The highest photon energy seen in the PL spectrum was 2.21 eV, independent of the excitation energy, cf. Sec. III A and Fig. 2. Consequently, the top of the upper PL-related band is 2.21 eV above the bottom of the lower PL-related band. In other words, $\varepsilon_1+\varepsilon_2+\varepsilon_3$=2.21 eV. Also, the minimum PL photon energy observed was 1.32 eV, and this must equal the band-gap energy ε_1 between the two PL-related bands. If E_3=0, as discussed above, then $\varepsilon_2=E_1-E_2-\varepsilon_1$=0.20 eV, and ε_3=2.21 eV $-\varepsilon_1-\varepsilon_2$=0.69 eV. The energy values are summarized in Table I.

In the absorption spectrum, Fig. 9, and also in all PLE spectra, Fig. 7, a kink is seen at 630 nm [(1.97±0.01) eV]. For photon energies above this energy, the rate of absorption for increasing photon energies increases more rapidly than below this kink. This amount of energy cannot readily be identified with a combination of energies given in Table I. However, it may indicate the location of a conduction band edge above the HOMO. This is in agreement with Ref. 41, according to which, the electrical band-gap energy for PS is 2.2 eV, whereas a value of 2.9 eV is given in Ref. 42. The determination of the electrical band gap with the use of photoconductivity is hampered by persistent photoconductivity, as well as slowly varying photoconductivity with time constants of several minutes or even hours.[43]

PS powders produced from different wafers and under different etching conditions had quite similar luminescence properties, which were not modified by mechanical crunching, cf. Sec. III A. Therefore, the energies given in Table I for PS powder, as related to the energy-band structure shown in Fig. 10, is basically sample independent.

The level structure shown in Fig. 10 is somewhat in accordance with models proposed,[44,45] according to which the excitation takes place in the bulk and the radiative recombination involves surface states. Thus, following such ideas, the band drawn at an energy E_1 above the HOMO in the left part of Fig. 10 would be of bulk nature, and the band-gap energy E_1 would consequently be the optical band gap for bulk PS. The two bands to the right in Fig. 10 would be surface-related bands. The structure shown in Fig. 10 fulfills the important condition specified in Ref. 45 that PL at a specified photon energy requires a larger excitation energy than that detected (cf. Fig. 8). Also, it is in accordance with the well-established fact that the PL from PS is generally found to be quite sensitive to surface conditions. This point will be discussed further at the end of this section. However, returning to the above-introduced distinction between bulk and surface, we find it difficult to specify what should be understood by bulk PS, because of the following. First, because the PS powder was freed from the Si wafer that it was grown on, the absorption and thus the band gap E_1 to the left in Fig. 10 cannot be related to properties of bulk silicon. Next, in the model outlined in Ref. 45, the PL emission should occur only from Si nanoparticles of size below 5 nm. However, PL has been observed from columns much larger than 5 nm (Ref. 46), in disagreement with the model presented in Ref. 45. Therefore, it is also problematic to relate the left of Fig. 10 to Si nanoparticles in the PS. Concerning the possibility of direct absorption into the surface state followed by emission, it seems problematic to incorporate that the band responsible for the absorption is extended to energies above the top of the upper PL-related band, as our PLE data indicate. One possibility is, that the left part of Fig. 10 reflects properties of a chemical compound, which in our etchings was formed in layers of sufficient thickness to possess bulk properties. We want to point out that the band diagram sketched in Fig. 10 is clearly qualitatively compatible with the diagram of the oxygen-defect-based model, as sketched in Ref. 14. However, here we shall not speculate further on the nature of the bands, because additional measurements are clearly required to clear up this point.

Concerning PS films, a similar energy-band diagram can be discussed in terms of data given in Fig. 8 and Sec. III A. The results are given in Table I. However, PS films prepared from different wafers and also under different etching conditions showed somewhat different PL properties. Also, for thick PS films, the luminescence is known to depend on the depth below the macroscopic surface.[47–49] Therefore, the energy values given in Table I for PS films are definitely more dependent on preparation than those given for PS powder. This is also accentuated by the data points in Fig. 8 for a heat-treated PS film, which for high detection energies resemble PS film, but for low detection energies come close to corresponding points for PS powder. At the same time, heat treatment caused the finer structure seen in the PL spectra at temperatures below 80 K to disappear, see Sec. III B and Fig. 7. This makes it possible to relate the finer structures to some intermediate version of PS, which during prolonged etching is processed further, as the PS film material is converted to PS powder. This interpretation is confirmed by Ref. 49, in which a free-standing PS film was created by etching the silicon wafer away from the back side of the wafer. Subsequently, both sides of the free-standing film were studied with PL, and whereas a fine structure almost identical to what we have observed was seen from the back side of the film (i.e., the lately created PS), no similar structure was seen

from the top surface of the film (i.e., where PS formation was initiated).

At least two different reactions can take place during the heat treatment carried out here, which resulted in the disappearance of the finer structures in the PL spectra at low temperatures. According to Ref. 11, hydrogen desorption takes place, and this enhances the PL intensity.[11] Thus, the intermediate version of PS may have a higher content of hydrogen than the PS powder, resulting in the finer structure and also that the PL from as-grown films is less intense than the PL from powder. Another possibility is, that since the heat treatment was carried out in air, oxidation could take place. It has been observed that oxidation of PS both enhances and stabilizes the PL efficiency.[50] Our SIMS measurements seemed to indicate that annealing reduced the content of hydrogen and also increased the content of oxygen. However, they were not quantitative enough to be conclusive. A correlation between PL and chemical composition for PS as-grown, as well as annealed at different temperatures up to 900 K has been reported in Ref. 51. Our samples have been produced at current densities above 10 mA/cm^2, which leads to hydrogen-rich samples.[51] Actually, the PL data obtained from our PS films conform well with corresponding results obtained from hydrogen-rich samples given in Ref. 51, whereas the PL data obtained from our PS powders are more blueshifted, indicating a reduced content of hydrogen.[51] Also, the heat treatment that we carried out on a PS film shifted the PL towards the blue at the same time as the finer structure seen at low temperatures in the as-grown film was removed (cf. Figs. 5, 6). By comparison to Ref. 51, this seems to indicate that the finer structure seen at low temperatures in as-grown films is related to presence of excess hydrogen (see Ref. 51 for details), which desorbs from the PS film during the heat treatment and which also disappears from the PS during prolonged etchings, which results in formation of PS powder. However, also here, further measurements are needed to clear up this point, which, albeit not necessarily being very important, at least is very fascinating.

Recapitulating briefly, the luminescence properties of PS powder seem to be satisfyingly reproducible and the energy-band structure of PS powder is summarized in Fig. 10 and Table I. PS films, on the other hand, seem to possess properties, which depend on the layer depth, or, in other words, on the degree of processing. Consequently, the energy-band structure for PS film, as sketched in Fig. 10 and with data given in Table I, can only be taken as a gross structure scheme, finer details will depend on the site of the PS in the film layer. Of all models proposed for the PL properties of PS, our data are compatible only with the oxide-defect-based model.[14,15]

ACKNOWLEDGMENTS

This work has been supported by the Danish Natural Science Research Council, the Danish National Agency of Technology, the Carlsberg Foundation, Director Ib Henriksens Foundation and the NOVO Nordic Foundation. All grants are highly appreciated. We want to thank most sincerely Dr. E. Johnson, Dr. I. Søndergaard, and Dr. Peixiong Shi for carrying out the transmission electron microscopy, the scanning electron microscopy, and the secondary-ion-mass spectroscopy, respectively.

[1] C. Pickering, M. I. J. Beale, D. J. Robbins, P. J. Pearson, and R. Greef, J. Phys. C **17**, 6535 (1984).
[2] L. T. Canham, Appl. Phys. Lett. **57**, 1046 (1990).
[3] A. Uhlir, Jr., Bell Syst. Tech. J. **35**, 333 (1956).
[4] D. J. Lockwood, Solid State Commun. **92**, 101 (1994).
[5] G. Bomchil, A. Halimaoui, I. Sagnes, P. A. Badoz, I. Berbezier, P. Perret, B. Lambert, G. Vincent, L. Garchery, and J. L. Regolini, Appl. Surf. Sci. **65/66**, 394 (1993).
[6] S. S. Iyer and Y.-H. Xie, Science **260**, 40 (1993).
[7] S. M. Prokes and O. J. Glembocki, Mater. Chem. Phys. **35**, 1 (1993).
[8] V. Lehmann and U. Gosele, Appl. Phys. Lett. **58**, 856 (1991).
[9] R. A. Street, Adv. Phys. **25**, 397 (1976).
[10] D. J. Wolford, B. A. Scott, J. A. Reimer, and J. A. Bradely, Physica **117/118**, 920 (1983).
[11] S. M. Prokes, O. J. Glembocki, V. M. Bermudez, R. Kaplan, L. E. Fridersdorf, and P. C. Searson, Phys. Rev. B **45**, 13 788 (1992).
[12] T. Motohiro, T. Kachi, F. Miura, Y. Takeda, S.-A. Hyodo, and S. Noda, in *Light Emission From Silicon*, edited by S. S. Iyer, R. T. Collins, and L. T. Canham, MRS Symposia Proceedings No. 256 (Materials Research Society, Pittsburgh, 1992), p. 53.
[13] M. S. Brandt, H. D. Fuchs, M. Stutzmann, J. Weber, and M. Cardona, Solid State Commun. **81**, 307 (1992).
[14] S. M. Prokes, W. E. Carlos, and O. J. Glembocki, Phys. Rev. B **50**, 17 093 (1994).
[15] S. M. Prokes and W. E. Carlos, J. Appl. Phys. **78**, 2671 (1995).
[16] L. N. Dinh, L. L. Chase, M. Balooch, L. J. Terminello, and F. Wooten, Appl. Phys. Lett. **65**, 3111 (1994).
[17] N. Andersen, K. Jensen, J. Jepsen, J. Melskens, and E. Veje, Appl. Opt. **13**, 1965 (1974).
[18] M. Stutzmann, M. S. Brandt, E. Bustarret, H. D. Fuchs, M. Rosenbauer, A. Höpner, and J. Weber, J. Non-Cryst. Solids **164-166**, 931 (1993).
[19] M. I. J. Beale, J. D. Benjamin, M. J. Uren, N. G. Chew, and A. G. Cullis, J. Cryst. Growth **73**, 622 (1985).
[20] R. L. Smith and S. D. Collins, J. Appl. Phys. **71**, R1 (1992).
[21] P. C. Searson, J. M. Macaulay, and S. M. Prokes, J. Electrochem. Soc. **139**, 3373 (1992).
[22] G. B. Amisola, R. Behrensmeier, J. M. Galligan, F. A. Otter, F. Namavar, and N. M. Kalkoran, Appl. Phys. Lett. **61**, 2595 (1992).
[23] V. P. Parkhutik, J. M. Albella, J. M. Martinez-Duart, J. M. Gomez-Rodriguez, A. M. Baro, and V. I. Shershulsky, Appl. Phys. Lett. **62**, 366 (1993).
[24] N. Ookuba, Y. Matsuda, Y. Ochiai, and N. Kuroda, Mater. Sci. Eng. B **20**, 324 (1993).
[25] T. Yu, R. Laiho, and L. Heikkilä, J. Vac. Sci. Technol. B **12**, 2437 (1994).
[26] I. M. Chang, G. S. Chuo, D. C. Chang, and Y. F. Chen, J. Appl. Phys. **77**, 5365 (1994).
[27] C. C. Klick and J. H. Schulman, in *Solid State Phys.: Advances in Research and Applications*, edited by F. Seitz and D. Turnbull (Academic, New York, 1957), Vol. 5, p. 97.

[28] G. C. John and V. A. Singh, Phys. Rev. B **50**, 5329 (1994).
[29] A. Venkatesware Rao, F. Ozanam, and J. N. Chazalviel, J. Electrochem. Soc. **138**, 153 (1991).
[30] S. M. Prokes and O. J. Glembocki, Phys. Rev. B **49**, 2238 (1994).
[31] N. Do, L. Klees, P. T. Leung, F. Tong, W. P. Leung, and A. C. Tam, Appl. Phys. Lett. **60**, 2186 (1992).
[32] C. Tsang and R. A. Street, Phys. Rev. B **19**, 3027 (1979).
[33] M. S. Brandt, A. Breitschwerdt, H. D. Fuchs, A. Höpner, M. Rosenbauer, M. Stutzmann, and J. Weber, Appl. Phys. A **54**, 567 (1992).
[34] M. Rosenbauer, M. S. Brandt, H. D. Fuchs, A. Höpner, A. Breitschwerdt, and M. Stutzmann, in *Optical Properties of Low Dimensional Structures*, edited by D. C. Bensahel, L. T. Canham, and S. Ossicini (Kluwer, Dordrecht, 1993), p. 43.
[35] S. L. Friedman, M. A. Marcus, D. L. Adler, Y.-H. Xie, T. D. Harris, and P. H. Citrin, Appl. Phys. Lett. **62**, 1934 (1993).
[36] Gmelin, *Handbuch der Anorganische Chemie* (Verlag Chemie, Weinheim, 1959), Vol. B, p. 594.
[37] M. S. Brandt, H. D. Fuchs, M. Stutzman, J. Weber, and M. Cardona, Solid State Commun. **81**, 307 (1992).
[38] M. Stutzmann, M. S. Brandt, M. Rosenbauer, J. Weber, and H. D. Fuchs, Phys. Rev. B **47**, 4806 (1993).
[39] M. Stutzmann, M. S. Brandt, M. Rosenbauer, H. D. Fuchs, S. Finkbeiner, J. Weber, and P. Deak, J. Lumin. **57**, 321 (1993).
[40] H. Ubara, T. Imura, A. Hiraki, I. Hirabayashi, and K. Morigaki, J. Non-Cryst. Solids **59&60**, 641 (1983).
[41] Z. Chen, Y.-Y. Lee, and G. Bosman, Appl. Phys. Lett. **64**, 3446 (1994).
[42] P. H. Hao, X. Y. Hou, F. L. Zhang, and X. Wang, Appl. Phys. Lett. **64**, 3602 (1994).
[43] T. Frello, O. Leistiko, and E. Veje, J. Appl. Phys. **79**, 1027 (1996).
[44] C. Delerue, M. Lannoo, and G. Allan, J. Lumin. **57**, 249 (1993).
[45] F. Koch, V. Petrova-Koch, and T. Muschik, J. Lumin. **57**, 271 (1993).
[46] P. B. Fischer, K. Dai, E. Chen, and S. Y. Chou, J. Vac. Sci. Technol. B **11**, 2524 (1993).
[47] N. Ookubo, J. Appl. Phys. **74**, 6375 (1993).
[48] G. Ambrazevicius, G. Zaicevas, V. Jasutis, D. Lescinskas, T. Lideikis, I. Simkiene, and D. Gulbinaite, J. Appl. Phys. **76**, 5442 (1994).
[49] J. Oswald, J. Pastrnak, A. Hospodkova, and J. Pangrac, Solid State Commun. **89**, 297 (1994).
[50] P. O'Keeffe, Y. Aoyagi, S. Komuro, T. Kato, and T. Morikawa, Appl. Phys. Lett. **66**, 836 (1995).
[51] L. Tsybeskov and P. M. Fauchet, Appl. Phys. Lett. **64**, 1983 (1994).